Time-Dependent CIDEP and ESR Observations in the Photochemical Systems Involving 1,3,5-Tris(3,5-di-*tert*-butyl-4-hydroxybenzyl)-2,4,6-methylbenzene (Irganox 1330)

I. A. Shkrob, Patrick Felder, and Jeffrey K. S. Wan*

Contribution from the Department of Chemistry, Queen's University, Kingston, Ontario, Canada K7L 3N6

Received September 15, 1992

Abstract: The 100-kHz and time-dependent TR ESR results on the photooxidation of 1,3,5-tris(3,5-di-*tert*-butyl-4-hydroxybenzyl)-2,4,6-trimethylbenzene (**IOH**) reveal that two radicals are formed. The experimental observations are consistent with the initial formation of the primary phenoxy radical **IO** which is broadened by fast **H**-exchange from one phenolic moiety to another. The second radical **XO** exhibits hindered rotation of its methylene group and is suggested to be produced from secondary photolysis of an intermediate photoproduct, likely **I═O**, formed via a self-disproportionation reaction of the **IO** radicals. It is proposed that the formation of a charge-transfer complex between the phenol group and the quinoidal group in the **I═O** moiety suppresses the **H**-exchange between the phenolic groups in the radical. The slowed down rotation of the methylene group in the **XO** radical is likely due to its bulky structure. No experimental evidence is found for the possible formation of diradicals in the **IOH** system.

1. Introduction

Phenols as a class of chemical compounds have long been an interesting subject of many chemical and industrial studies. The most common application of substituted phenols in industry is perhaps their utility as antioxidants. The remarkable antioxidation properties of these phenols are largely associated with the facile phenolic hydrogen abstraction and their effective scavenging of peroxy and alkoxy radicals, which are the main reactants in autooxidation. In some cases the intermediate phenoxy radicals may undergo further oxidation, leading to quinoid products. For example, the free-radical oxidation of methoxy-substituted phenoxy radicals has recently been demonstrated as a major mechanism in the photoinduced yellowing of pulp and paper;[1] furthermore, it is generally agreed that a substantial proportion of the yellowing is due to the formation of *o*-quinones from the phenoxy radical intermediates. Our current interests, however, focus more on the chemical and physical properties of some of these intermediate phenoxy radicals.

One of the popular commercial antioxidants, Irganox 1330 by Ciba-Geigy, is 1,3,5-tris(3,5-di-*tert*-butyl-4-hydroxybenzyl)-2,4,6-trimethylbenzene (**IOH**). It is a large trifunctional phenol with an interesting symmetrical structure as represented below:

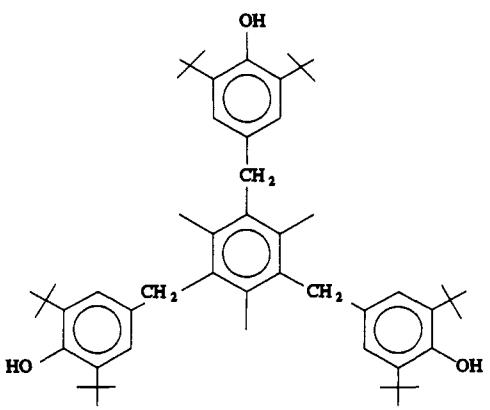

IOH

Earlier ESR studies of polyphenolic compounds[2,3] were generally concerned with the aspects of spin delocalization over an extended conjugated system and the interesting observation of triplet diradical species such as Yang's biradical[2] in glassy matrices. However, very little is known about the chemistry of the polyphenolic radicals and their dynamic properties as studied by time-resolved ESR techniques. At first thought, the hindered structure of **IOH** would suggest that it might yield relatively persistent or stable phenoxy radicals which could afford the interesting possibility of producing diradicals or even triradicals in solution.

However, experiments using conventional methods for generating phenoxy radicals resulted in the observation of 100-kHz spectra with line intensities which deviated substantially from the expected 1:2:1 pattern caused by the methylene proton coupling. Further TR ESR studies of **IOH** were undertaken which revealed a wealth of radical dynamic processes and chemistry. The technique of TR ESR is uniquely suited to probe the time-dependent behaviors of transient radicals as exhibited in the evolution of their chemically induced dynamic electron polarizations (CIDEP) with time. The complex trifunctional and hindered stereochemical structure of Irganox 1330 provides significant possibilities for the observation of the effects of processes such as hindered rotation and exchange effects via dynamic spectral changes.[4,5] In time-resolved ESR studies, the phenomenon of hindered rotation on the spectral dynamics has only been reported once previously,[5] and the effects of chemical exchange accompanied by hindered rotation in polarized radicals have not been dealt with in detail. It is important that such effects be consistently predicted in both modulated ESR spectra and CIDEP spectra. We have therefore undertaken such a study using Irganox 1330; a theoretical treatment of these effects is presented in the final section of this article.

Additionally, the intriguing question of the possibility of diradical formation and observation remains. In a large molecule such as **IOH**, the two unpaired spins may be so far apart that

(1) Wan, J. K. S.; Tse, M. Y.; Shkrob, I. A.; Depew, M. C. In *Photochemistry of Lignocellulose Materials*; Heitner, C., Scaiano, J. C., Eds.; ACS Symposium Series, in press.

(2) Mukai, K.; Hara, T.; Ishizu, K. *Bull. Chem. Soc. Jpn.* **1979**, *52*, 1853, 1911.

(3) Kothe, G.; Nowak, C.; Denkel, K.-H.; Ohmes, E.; Zimmermann, H. *Angew. Chem., Int. Ed. Engl.* **1970**, *9*, 520.

(4) McLauchlan, K. A. In *Modern Pulsed and Continuous-Wave Electron Spin Resonance*; Kevan, L., Bowman, M. K., Eds.; Wiley Interscience: New York, 1990; p 285.

(5) McLauchlan, K. A.; Stevens, D. G. *J. Chem. Phys.* **1987**, *87*, 4399.

0002-7863/93/1515-5227$04.00/0

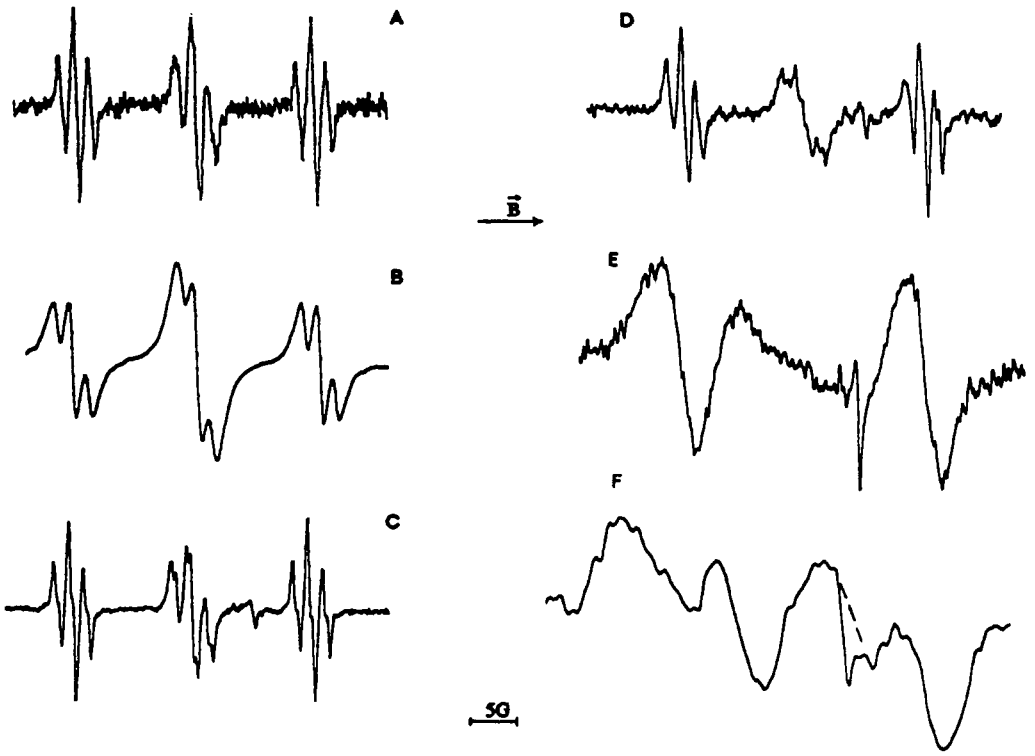

Figure 1. ESR spectra (100 kHz) in the direct laser photolysis of **IOH** in toluene solutions without triplet initiators. (a and b) Broadening of lines with increasing flow rates: (a) 0.3 mL/h; (b) 0.3 mL/min. (c–f) Changes in the spectral appearance at different temperatures: (c) –40 °C; (d) –55 °C; (e) –105 °C; (f) –110 °C (frozen matrix).

their interaction is negligible, and thus the diradical may exhibit hyperfine splittings/patterns nearly identical to those of the monoradicals. However, it was found that the primary **IO** phenoxy radicals are rather reactive, and it was therefore surprising that experimentally no evidence was detected that diradicals derived from **IOH** were present, even in solid matrix at 77 K.

2. Experimental Section

The 100-kHz modulated and TR ESR spectra were obtained simultaneously during the laser photolysis of toluene solutions of Irganox 1330, **IOH** (Ciba-Geigy, used twice recrystallized from EtOH), and respective photoinitiators: benzophenone (BP), benzophenone-d_{10} (BP), acetophenone (AP), flavone (FV), 2-acetylfuran, *tert*-butyl peroxide (TBP), pyruvic acid (PA), duroquinone (DQ), benzoquinone (BQ), 2,5-diphenylbenzoquinone, chloranil, and fluoranil, all from Aldrich. For experiments in acidic media, solution pH was adjusted by adding glacial acetic acid to the toluene solutions. Measurements in basic media were performed in methanolic solutions containing a certain amount of sodium methylate. As well, ethanolic and toluene–decalin and toluene–triacetin solutions were used in order to increase the bulk viscosity of the solutions.

Simultaneous 100-kHz (thermalized) and TR ESR (polarized) spectra[6] were obtained either on a Varian E103 spectrometer using a Lambda Physik EMG101-MSC Xe/Cl excimer laser (308 nm, 50 mJ/pulse, 10 Hz) or a Bruker spectrometer equipped with a Quanta Ray GCR-11 NdYag (355 nm, 60 mJ/pulse, 10 Hz). Some 100-kHz modulated spectra were also obtained separately with a 200-W super pressure mercury lamp as the radiation source. Diode signals were amplified and processed with a Stanford Research SR240 preamplifier coupled with a SR250 gated integrator, controlled by a computer via a SR245 interface. Typical field resolution was 500 points per 40 G, each field point representing an average of 20 shots. In order to minimize the broadening effects due to the simultaneous 100-kHz field modulation in TR ESR spectra, modulation amplitudes of <0.1–0.2 G (or none) were used. For some systems the evolution of magnetization was determined with 256 traces on and off resonance first stored in a Hitachi VC-6023 digital oscilloscope and then numerically subtracted.

The photolysis was performed in suprasil quartz cuvettes, 0.5-mm (Varian) and 4-mm cylindrical cells (Bruker); low-temperature measurements were carried out in a 3-mm cylindrical cell (Varian). Photolyses with chlorine as initiator were conducted in 4-mm Pyrex tubes containing toluene solutions saturated with the gas. All other solutions were deoxygenated either by purging with nitrogen or degassing by a few freeze–thaw cycles under vacuum.

A molecular mechanics study of Irganox 1330 was performed using the AMBER computer package supplied by Hyperchem (Autodesk, Inc.).[7]

3. Results and Discussion

(a) ESR Spectra. Irradiation of **IOH** solutions in the presence of various triplet initiators results in the observation of ESR spectra consisting of a triplet of triplets with rather abnormal intensities but with coupling constants (13.4 and 1.73 G) very similar to those of comparable 2,6-di-*tert*-butyl-4-alkylphenoxy radicals (Figures 1–3). Moreover, the spectral features were found to be dramatically dependent upon the flow rate of reagents, the temperature, the operating conditions of the pulsed laser (intensity, frequency, and the repetition rate), and especially the type of the photoinitiator. We shall consider these variations in a systematic way.

(*i*) Observation of CW-ESR spectra after direct photolysis at 308 nm of **IOH** in toluene solution is possible without the presence of triplet initiators, as was already performed for hindered monophenols.[8] No polarization (caused by excited triplet ^{3}**IOH**) was detected in our system under these conditions. The CW-ESR spectra, recorded at room temperature and at very low flow rates of the sample solution (<0.4 mL/h), exhibit an unusual 1:1:1 pattern of three line groups, split by 13.4 G (Figure 1a). Related to this appearance, a concomitant *alternating line width* occurs, manifested in the greater width of the three central lines than of the outer ones. However, on increasing the sample flow rates, the lines of all three groups broaden homogeneously (Figure 1b) and steadily. This homogeneous line broadening, coming

(6) Kam, E.; Craw, M. T.; Depew, M. C.; Wan, J. K. S. *J. Magn. Reson.* **1986**, *57*, 556.

(7) Weiner, S. J.; Kollman, P. A.; Case, D. A.; Chandra Singh, U.; Ghio, C.; Alagona, G.; Profeta, S., Jr.; Weiner, P. *J. Am. Chem. Soc.* **1984**, *106*, 765.

(8) Depew, M. C.; Emori, S.; Wan, J. K. S. *Res. Chem. Intermed.* **1989**, *12*, 275.

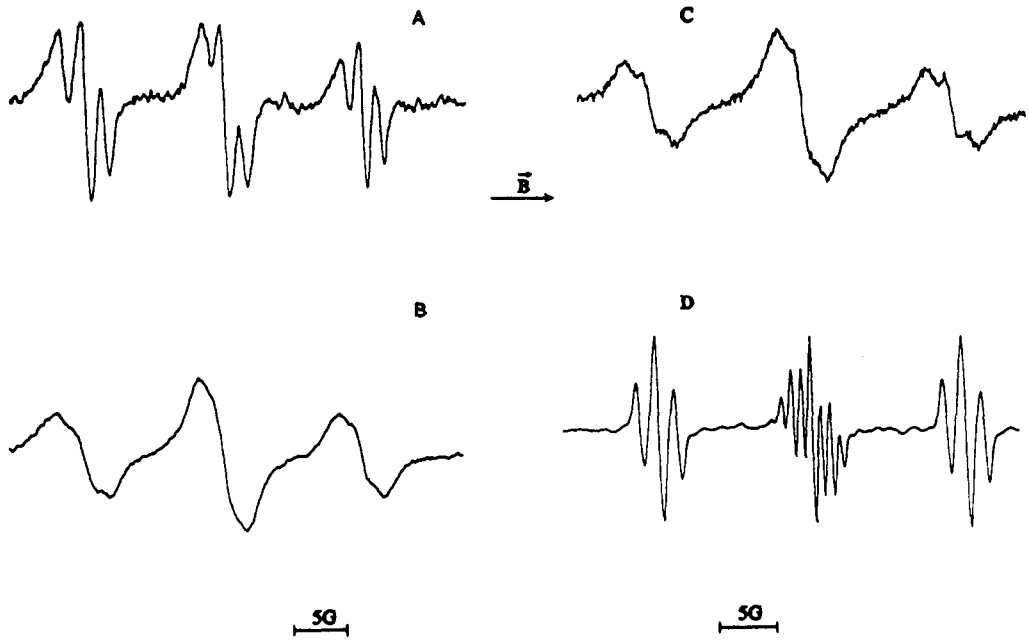

Figure 2. ESR spectra (100 kHz) in the direct laser photolysis of **IOH** in toluene solutions containing triplet initiators: (a–c) duroquinone (355 nm) and (d) acetophenone (308 nm). Changes in the spectral appearance (a,b) are observed on increasing the flow rate of acidified toluene solutions. Without acid (c), the spectral shape is flow-independent. When AP is used as initiator, the spectra (d) are not dependent on the flow rate and acidity of the solutions.

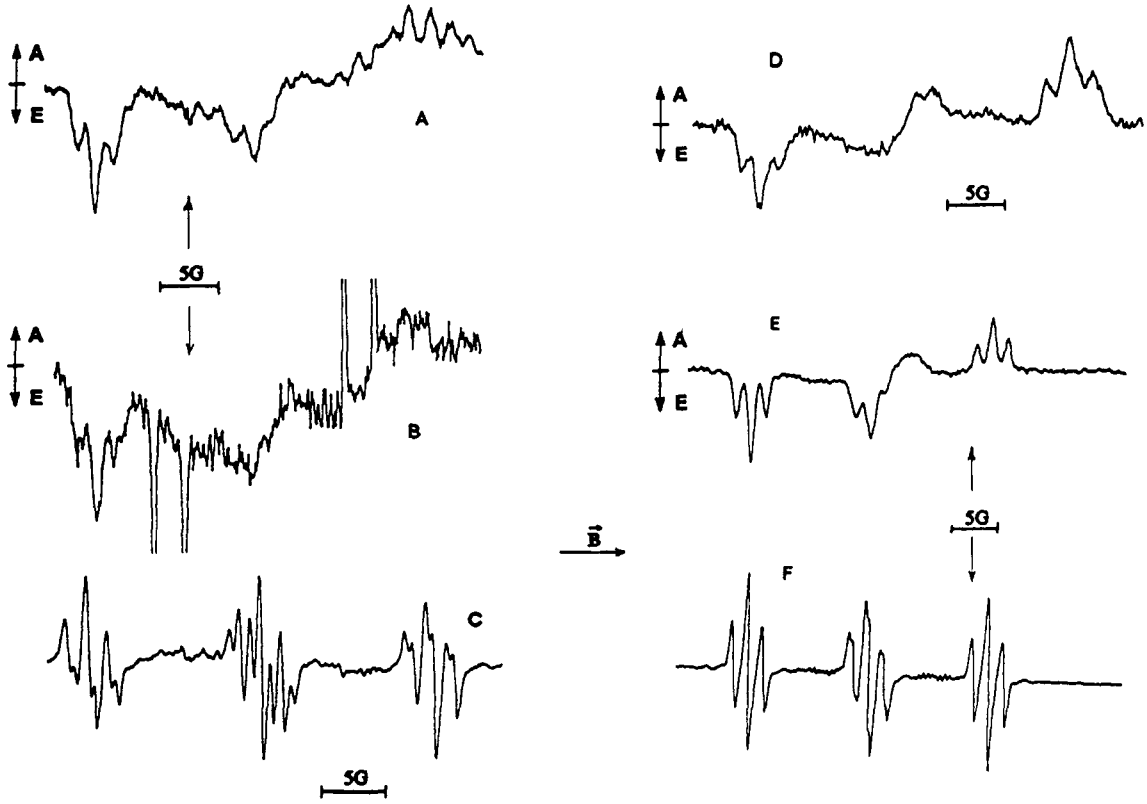

Figure 3. Variations in the spectral appearance using different triplet initiators: (a) TR ESR spectrum from 2-acetylfuran/**IOH**/toluene solution (308 nm, 0.3–0.6 μs); (b and c) TR and 100-kHz spectra from pyruvic acid/acetic acid/**IOH**/toluene solution (308 nm, 1–2 μs); (d) TR ESR spectra from flavone/**IOH**/toluene solutions (355 nm, 3.5–5.5 μs); and (e) TR ESR spectra from benzophenone-d_{10}/**IOH**/toluene solutions (308 nm, 0.3–0.6 μs). For comparison, the simultaneously recorded 100-kHz ESR spectrum is given in f.

from a source other than the alternating line width effect, is accompanied by an increase in intensity of the central group, leading to a more 1:2:1-like pattern.

The alternating line width effect becomes more apparent on lowering the temperature. Below about 0 °C, the intensity of the central multiplet clearly decreases and broadens relative to that of the outer ones (Figure 1c–e). At −105 °C, the central group disappears and begins to split into two groups (Figure 1e). In frozen toluene matrix at temperatures below −110 °C, these two groups are clearly separated in the spectra (Figure 1f). Unfortunately, in the temperature-dependence experiments (Figure 1c–f), a quartz dewar had to be used which gave rise to a signal appearing between the central group and the one at higher external field. When the experiments in frozen matrix were performed,

scans over 200 G with high modulations (4–8 G) gave no indications of the presence of triplet diradicals, not even at 77 K. Therefore, it is concluded that the observed splitting pattern of a doublet of doublets stems from the couplings of the two chemically inequivalent methylene protons. This nonequivalency is due to drastically decreased (internal) rotation of the methylene group in toluene matrix. Although the higher contribution of anisotropy under these conditions does not allow the determination of the exact values of the two coupling constants, they were estimated to be 6 and 21 G, respectively. However, in the temperature range from 10 °C up to 60 °C, the spectra remained essentially unchanged.

In the temperature range between –20 °C and –60 °C, an increase in the number of lines is observable. Each central line is split into three lines, while the number of lines in the wings is doubled. This is due to a superposition of two spectra as is explained in further detail later in the text.

(*ii*) When aromatic ketones (BP, AP, FV) in toluene at 20 °C were used as initiators (308- or 355-nm excitation), the spectra resembled a 1:1:1 pattern, with at times a characteristic increase in the number of lines in the central group (Figures 2d and 3f), similar to the spectra in Figure 1c,d. The main features of these spectra were essentially independent of the flow rates and the laser properties; these results are not surprising taking into account that the signals persisted for several minutes after the photolysis, indicating that the observed radical was very stable.

However, the relative intensities of the signals were found to be dependent on the solution viscosity. For example, addition of paraffin oil or triacetin to the solution led to broadening of the central line with an accompanying progressive reduction of its relative intensity as the solution viscosity increased. This intensity reduction was, however, reversed on further increase in viscosity by adding decalin, due to homogeneous broadening of all lines. The intensity of the central multiplet was also observed to decrease at low temperatures.

Addition of acetic acid produced no changes in the spectral shape. However, the addition of $NaOCH_3$ to a methanolic solution of BP/**IOH** decreased the signal gradually and the lines from the BP anion radical appeared. When the solution was made sufficiently basic for the deprotonation of all three hydroxy groups, the characteristic spectrum collapsed into a very weak triplet (1.5 G). Similar results were obtained for the BP-d_{10}/**IOH** system and for the alkaline solution of **IOH** alone.

(*iii*) However, quite different results were obtained with initiation of photolysis at 355 nm by DQ and other quinones (benzoquinone, 2,5-phenylbenzoquinone, chloranil, and fluoranil). In the neutral solutions with these initiators, all the lines were very broad (ca. 1.5–2 G) and near 1:2:1 in relative intensity, independent of the flow rates (Figure 2c). In acidic solutions with comparable flow rates, the spectra were considerably narrower in line width and were of 1:1:1 character (Figure 2a). This effect appeared to be correlated with the pK_a of the corresponding semiquinone radicals, being minimal for halogen-substituted quinones and maximal for DQ. In contrast to the neutral solutions, a pronounced flow dependence in acidic DQ solutions was observed: at high flow rates the spectrum was 1:2:1 with broad lines (Figure 2b), while at slow flow (or no flow at all) it was of 1:1:1 character (Figure 2a). A similar homogeneous broadening and conversion from 1:1:1 to 1:2:1 appearance as the flow rate increased was also obtained when TBP was used as an initiator (Figure 4a); at the slow flow rates the spectra closely resembled those observed for BP/**IOH** system. In a parallel study, when **IOH** was replaced by 2,6-di-*tert*-butylcresol, the signal gradually decreased as the concentration of TBP was depleted at 355 nm. However, this was not the case with 2,4,6-tri-*tert*-butylphenol. It is likely that this difference is due to the fact that phenoxy radicals from the latter phenol are not as reactive in

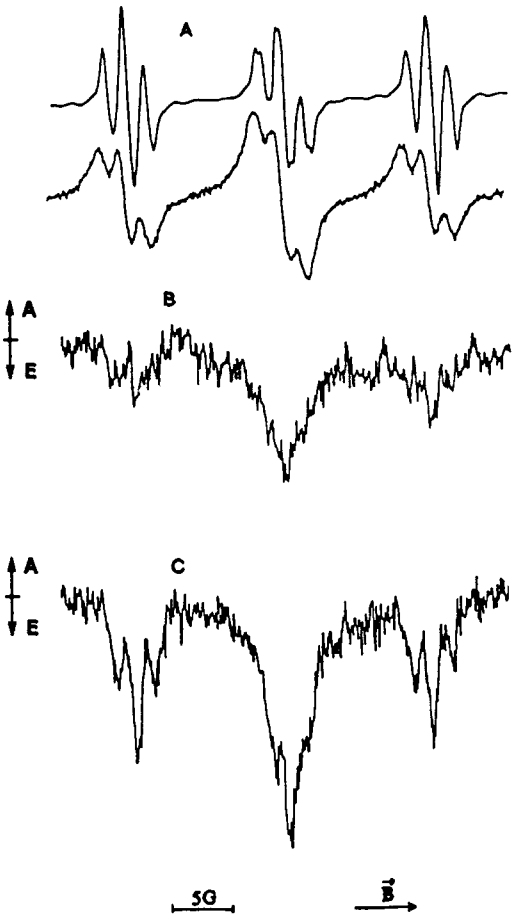

Figure 4. Spectra observed in TBP/**IOH**/toluene solutions (308 nm): (a) broadening of lines with increasing flow rates; (b and c) TR ESR spectra detected at (b) 0.2–0.5 μs and (c) 0.5–1 μs; at longer delay times spectra become more 1:1:1 in character (cf Figure 7d,e).

self-disproportionation reactions. This suggests that the products of disproportionation may play a key role in the secondary reactions.

Pyruvic acid was used as one of the triplet initiators in the **IOH** photolysis since its large α-methyl hyperfine coupling constant fortuitously avoids overlap with the central lines from the phenol spectrum. An extremely well resolved spectrum was observed with PA as initiator with additional hyperfine splittings (7 or 9 lines) seen not only in the central group but also in the wings (Figure 3c).

In addition to the aforementioned triplet photosensitizers, methods to generate the phenoxy radicals of **IOH** by several other routes were examined.

(*iv*) For example, using the 2,2-diphenyl-1-picrylhydrazyl radical (DPPH), the phenoxy radical can be generated in a thermal reaction. In this system a broad 1:2:1 triplet ESR spectrum was observed (Figure 5a) which resembled the detected spectra during the photooxidations by quinones and TBP at high flow rates.

(*v*) Photolysis of toluene solutions of **IOH** with added chlorine were also examined. After photolysis at 308 nm, a significant reduction in the intensity of the central multiplet, which was a function of the initial concentration of chlorine and the flow rates, was observed (Figure 5b,e). At slow flows of the chlorine-saturated solutions, the central line actually disappeared from the spectra.

(*vi*) In a comparative study of the photolysis of BP/phenol/**IOH** system in toluene, with phenol being in 60-fold excess relative to **IOH**, TR ESR results showed that in the first 5 μs after the laser flash only the BP ketyl radicals and the unsubstituted phenoxy radicals were observed (Figure 5g). Subsequently, it

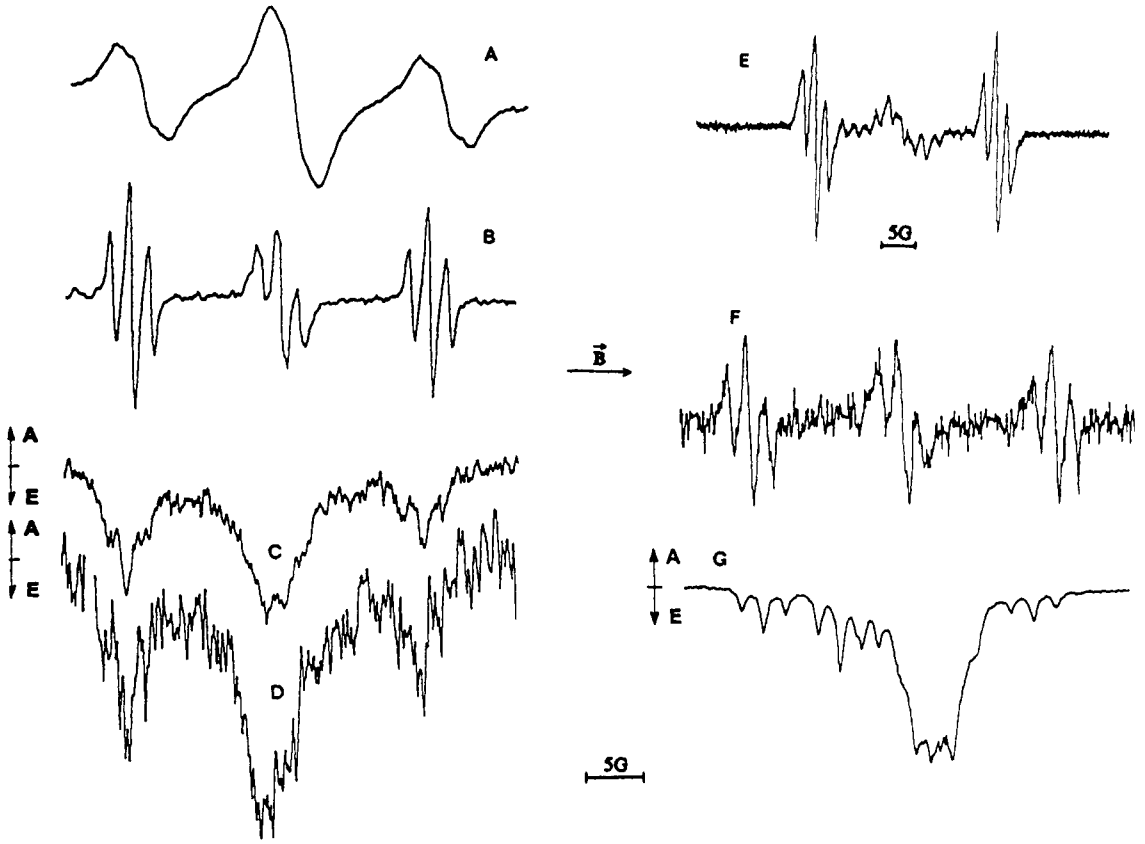

Figure 5. Other methods of generating radicals from **IOH**. (a) ESR (100 kHz) recorded immediately after addition of DPPH to **IOH**/toluene solutions. (b–e) Photolysis (308 nm) of **IOH**/toluene solutions containing chlorine. (b and e) Disappearance of the central group in the 100-kHz spectra as a function of chlorine concentration. (c and d) Simultaneous TR ESR spectra recorded at (c) 0.5–0.85 μs and (d) 0.2–0.7 μs. (f) The 100-kHz ESR spectrum in BP-d_{10}/**IOH**/phenol/toluene solutions containing 60-fold excess of phenol (308 nm). (g) Simultaneous TR ESR spectra recorded at 0.3–0.6 μs. At early stages only phenoxy radicals are observed with the 1:1 pattern characteristic of the 100-kHz spectrum.

was expected that the **IO** radicals would be formed by a secondary hydrogen abstraction reaction by the PhO radicals. However, the 100-kHz modulated ESR spectrum showed only a weak but clearly 1:1:1 spectrum as seen in Figure 5f. The same result was obtained when PhOH was replaced with hydroquinones.

At this point the foregoing observations appear to be rather confusing. However, it is apparent that at least two radical species are responsible for the features displayed in the 100-kHz ESR spectra. Both these radicals are phenoxy in nature, and their hfcc and *g*-factors are very similar to those of the phenoxy radical derived from di-*tert*-butylcresol.[9] Using the media effects and the variations of laser frequency allowed us to separate the relative contributions of these two radicals; the experimental observations indicate that (a) the generation of the radicals responsible for the well-resolved 1:1:1 pattern (the ones with an increased number of lines included) is a multistep process occurring on the time scale of seconds and (b) another species, exhibiting an extreme (up to 2 G) broadening under certain conditions, appears to be produced at a considerably faster rate. This homogeneous line broadening, which may be due to a variety of factors including hydrogen exchange and poor averaging of the hfi tensor in viscous solutions, appears to be correlated with the observation of the more 1:2:1-like pattern. Under certain experimental conditions, significant reductions in the relative intensity of the central group beyond the 1:1:1 ratio occur, even to the point of its total disappearance. This phenomenon is consistent with the effect of a hindered rotation in the methylene groups of the *o*-di-*tert*-butylphenol moieties.

Figure 6 shows a simplified reaction scheme proposed to account for some of the observations. The primary phenolic radical formed, **IO**, is suggested to have lines (homogeneously) broadened by H-exchange among the phenolic groups. The lack of an effect due to media acidity in the experiments (except in the quinone/**IOH** systems) suggests that the possible participation of ionized radical species and their accompanying degenerate electron exchange as an origin of the broadening are unlikely. It is further proposed that rapid formation of a secondary phenolic product, denoted **XOH** occurs; subsequent photolytic oxidation of this species yields a much more stable radical species, **XO**, which exhibits sharp spectral lines.

This scheme is consistent with the observations of spectral broadening and 1:2:1 appearance at fast flows, when **IO** predominates. At slower flows further conversions to **XO** occur and a sharp 1:1:1 spectrum superimposed on the weak and broad spectrum of the primary **IO** radicals is observed. Consequently, after photolysis the primary radicals decay rapidly and only the long-lived **XO** radicals remain. Thus, although in the systems with DPPH (Figure 5a), or DQ (Figure 2c) the primary radical can be seen, in most instances the secondary photolytic reactions proceed fast enough to provide a predominance of the **XO** radicals, and even if H-exchange in **IO** radicals is suppressed they may not be observable without time-resolved detection.

In the photolysis of TBP/**IOH** systems we observed a steady-state concentration of radicals even with no flow, which suggests that one of the potential products is the quinoid product **I=O** formed via disproportionation of the primary **IO** radicals. This quinoid product **I=O** is also photoactive toward both **IOH** and **XOH**.

In the experiments of quinone/**IOH** systems, the formation of **XOH** is slowed down in neutral solution compared to the other above-mentioned systems. We have no clear explanation for this behavior at this time. However, the effect of the acid in these

(9) Shkrob, I. A.; Depew, M. C.; Wan, J. K. S. *Res. Chem. Intermed.* **1992**, *17*, 271.

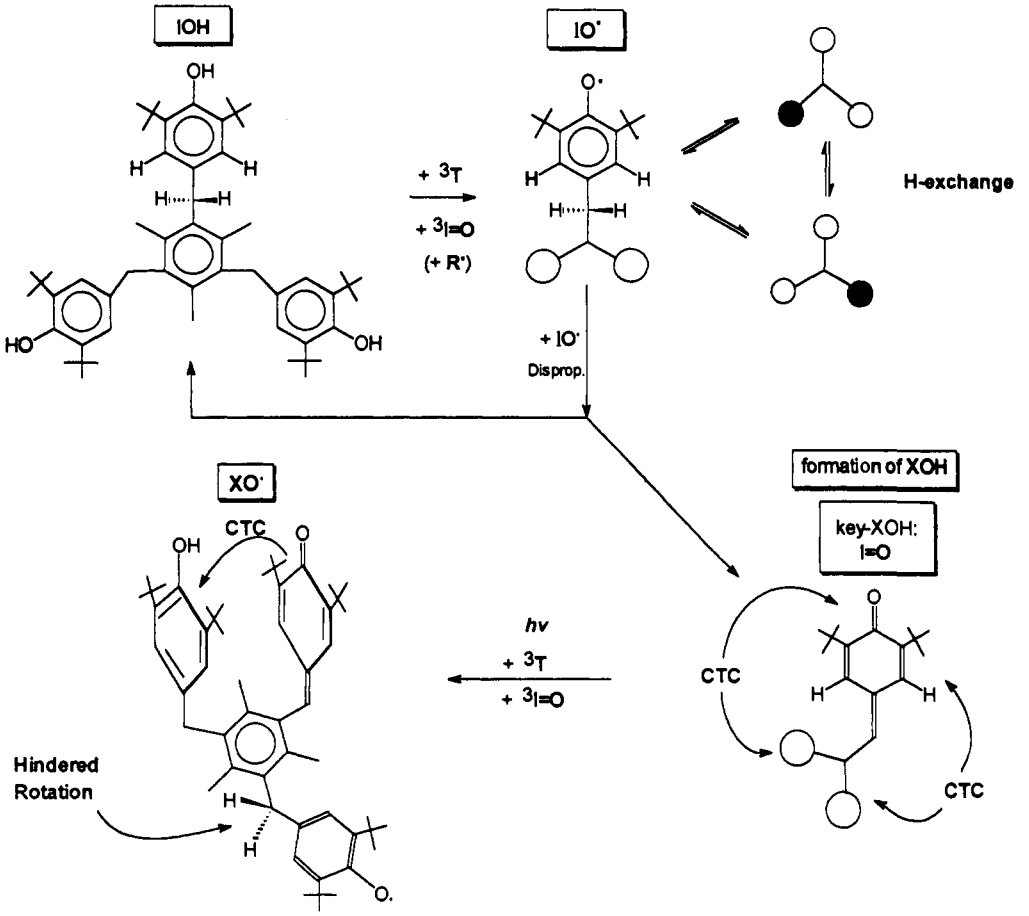

Figure 6. Proposed overall (primary and secondary) reaction scheme for the photolysis of **IOH**.

systems seems to be an enhancement of the reformation of quinone via self-disproportionation of semiquinone radicals. This in turn enhances the secondary photolysis of **XOH** with quinone to yield the **XO** radicals.

The molecular mechanics study performed showed that for **IOH** the molecular conformation with two parallel phenolic groups is energetically favored (being just 8 kJ/mol above the most thermodynamically stable C_{3v} conformation). In this conformation, the phenolic planes are separated by ca. 5–6 Å (Figure 7a). We suggest that such a conformational arrangement of two planar structures may also account for the proposed (intramolecular) fast **H**-exchange in the **IO** radical. (It is interesting to note that 1:1 hydrogen-bonded complexes between the hindered 2,4,6-tri-*tert*-butylphenoxy radical and various substituted phenols have previously been proposed as intermediates during the rapid hydrogen atom transfer reactions between these species. Such a mechanism accounted for the abnormally low activation energy barriers observed for the hydrogen atom transfer between oxyl radicals and was consistent with the observed preexponential factors[10]).

For the radical **XO**, the interaction between the quinone moiety and the phenol group may be stronger than the phenoxy–phenol interaction, since phenols are well known to form fairly stable CT-complexes with quinones.[11] Such a phenol–quinone complexing interaction would slow down the exchange between the phenoxy group and the remaining phenolic group (Figure 6), leading to our observation of a spectrum with quite sharp lines (however affected by hindered rotation and, in some cases, consisting of two superimposed components). This complexed radical structure is a better assignment for the proposed **XO** radical than a dimer since dimerization would be expected to be rather ineffective due to significant steric hindrance; it is also not clear why a dimer, if formed, would not be subjected to **H**-exchange similarly to the primary radical. With chlorine photoinitiation, the reactions are suggested to proceed much further, leading to the formation of diquinoid phenoxy radicals or, by addition or condensation reactions, to even bulkier radicals. The stronger complexing and/or higher steric hindrance in these radicals causes greater rotational barriers of the methylene groups, resulting in a characteristic 1:0:1 spectrum.

However, the question of why stronger rotational hindrance occurs in **XO** than in other alkyl-substituted phenoxy radicals still remains.

The observations under low-temperature conditions (frozen matrix) in which the spectrum shows a splitting pattern of only a doublet of doublets (Figure 1f), caused by the hyperconjugative coupling of the two methylene protons (couplings from the two *m*-positioned **H** not resolved), suggests that there are two energetically favored conformations, each with methylene protons in two magnetically nonequivalent sites, **1** and **2**. Therefore, the hindered rotation can be treated as a two-jump process during which the two sites are interconverted.[12] k_{12} and k_{21} are the rates of interconversion from **1** to **2** and **2** to **1**, respectively. If the two conformations are energetically equal, then $k_{12} = k_{21}$ ($= k$). In the case of the fast interconversion ($k > 10^{11}$ s^{-1}), the methylene protons become magnetically equivalent. As the experiments show a clear temperature-dependence (Figure 1c–f) of this rotation (or interconversion), an Arrhenius plot should provide quantitative information about the hindrance. By simulation of the exper-

(10) Mahoney, L. R.; DaRooge, M. A. *J. Am. Chem. Soc.* **1970**, *92*, 890; **1972**, *94*, 7002.

(11) Berger, S.; Hert, P.; Reiker, A. In *The Chemistry of Quinoid Compounds*; Patai, S., Rappaport, Z., Eds.; J. Wiley and Sons: New York, 1988; Vol. 2, Part 1, Chapter 2, p 29.

(12) von Borczyskowski, C.; Möbius, K.; Plato, M. *J. Magn. Reson.* **1975**, *17*, 202. Plato, M.; Biehl, R.; Möbius, K.; Dinse, K. P. *Z. Naturforsch.* **1976**, *31A*, 169.

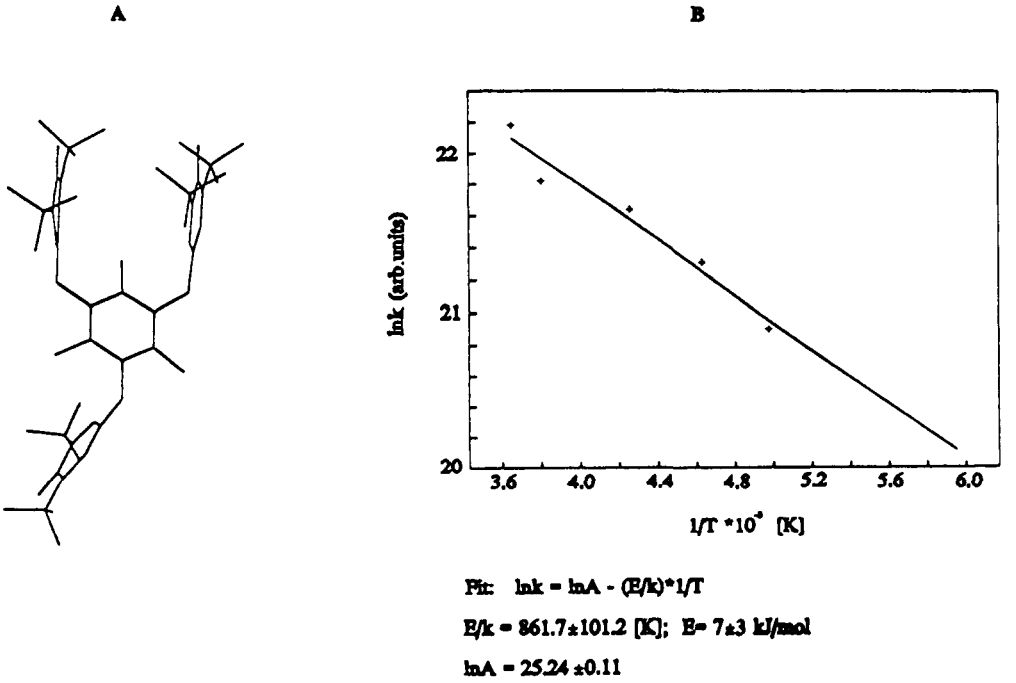

Figure 7. (a) One of the **IOH** conformations of lowest energy as simulated with AMBER. (b) Arrhenius diagram of the methylene jumping rate constants $k = k(T)$. See text for details.

imental CW-ESR spectra we obtained the rate constant k ($= k_{12} = k_{21}$) as a function of temperature. The unperturbed line widths required for this procedure at the various temperatures (five values between 0 °C and −70 °C) were taken from the lines of one of the outer groups. However, at temperatures below −20 °C the spectra were superimposed to an increasingly greater extent by a second component. Additionally, at decreasing temperatures, a rapid broadening of the central lines of both components accompanied by a decrease of their amplitudes took place, resulting in one unresolved hump at $T < -55$ °C. No fits for the individual components were possible and, therefore, the $k(T)$ values (of the first component) were estimated from the overall decrease of the central hump. Figure 7b shows the Arrhenius plot of $k = k(T)$. The linearity of the plot shows that we are dealing with a thermally activated process describable by $k = A^* \exp(-E/kT)$. The activation energy E and the preexponential factor A are estimated:

$$E \approx 7 \pm 3 \text{ kJ/mol} \quad \text{and} \quad A \approx 9 \times 10^{(10\pm0.5)} \text{ s}^{-1}$$

In spite of the errors introduced in the plot due to superposition of the spectra, the low value of the estimated energy barrier indicates that there does not exist a pronounced steric hindrance in **XO** and, hence, also not in **IO** (and **IOH**). The fact that there are no visible changes in the spectral appearance between 10 °C and 60 °C confirms a low energy barrier, as even a huge increase in temperature would result in only a small increase of the rate constant k (and, consequently, a small increase of the relative intensity of the central multiplet). The low preexponential factor is likely due to the "rigid" molecular structure. The bulky and inert fragments attached to the methylene groups slow down internal rotation and the overall flexibility. Although this behavior most probably would be the same for **IO** (and **IOH**), we have no real experimental evidence for slowed interconversion in the case of **IO**, since its spectral appearance is accompanied with homogeneous line broadening.

As our simulations show, the rate of rotation between the **XO** conformers (Figure 8) needed for the transformation of a 1:2:1 spectrum to the 1:1:1 spectrum (with an observed line width of about 0.3 G) is in the range of $(0.5–1) \times 10^{10}$ s^{-1}, which is only 10–15 times smaller if the rotation is fast. The corresponding estimate of the maximum barrier of the rotation is <50 kJ/mol, which is comparable to the energies of hydrogen bonding.

In the case of $k_{12}/k_{21} \neq 1$ (i.e., when a certain orientation of the methylene group prevails) both the 100-kHz ESR and CIDEP spectra will be different from the case examined above. The central group splits in two, and at fast exchange, $k_{12,21}$ ca. $(0.1–1) \times 10^{12}$ s^{-1}, a 1:1:1:1 spectrum becomes apparent (Figure 8c). The difference in field position of the two central groups is then only dependent on the ratio of $k_{12}/k_{21} \neq 1$. The aforementioned superimposed second component in most of the well-resolved 100-kHz ESR spectra can be simulated with slightly different values of k_{12} and k_{21}, as the two central groups are separated by only ≤1.7 G in all cases of their observation; k_{12} and k_{21} are in the range of $(0.1–1) \times 10^{11}$ s^{-1}. If the two groups are separated by ≈1.7 G (same splitting as the *m*-protons), a central "quartet" appears. We attribute this additional component to another secondary phenoxy radical, denoted **X'O**. The lowered symmetry which manifests itself in the slightly different rates of interconversion must be due to a more complex structure, favoring one conformer. The spectra show a similar temperature dependence of **X'O** and **XO**.

The corresponding TR ESR spectra of the primary **IO** and secondary **XO** should also exhibit the same homogeneous and alternating line broadening phenomena.[4,13] Therefore, TR ESR observations given in the next section are a major test of the proposed scheme.

(b) Time-Resolved ESR Observations. TR ESR spectra observed in the laser photolysis of **IOH** in toluene solutions containing, respectively, BP, BP-d_{10}, PA, 2-acetylfuran, and flavone are shown in Figures 3–5. In most of the spectra two components in addition to the signals from the ketyl radicals of the triplet initiators are observable. The well-resolved component is due to the phenoxy radical, **XO** (e.g., Figure 3e), and the other consists of a broad (30 G wide) and unresolved signal (Figure 3a,b) which was attributed to **IO**.

The former radical signals were E^*/A polarized, with a major contribution (60–70%) from the antiphase (−1:0:1) component, reaching 100% in the flavone/**IOH** system (Figure 3d). This dominance of the RPM contribution is rather atypical for the alkyl-substituted phenols and hydroquinones, for which TM-

(13) McLauchlan, K. A.; Hore, P. J. *Mol. Phys.* **1981**, *42*, 533.

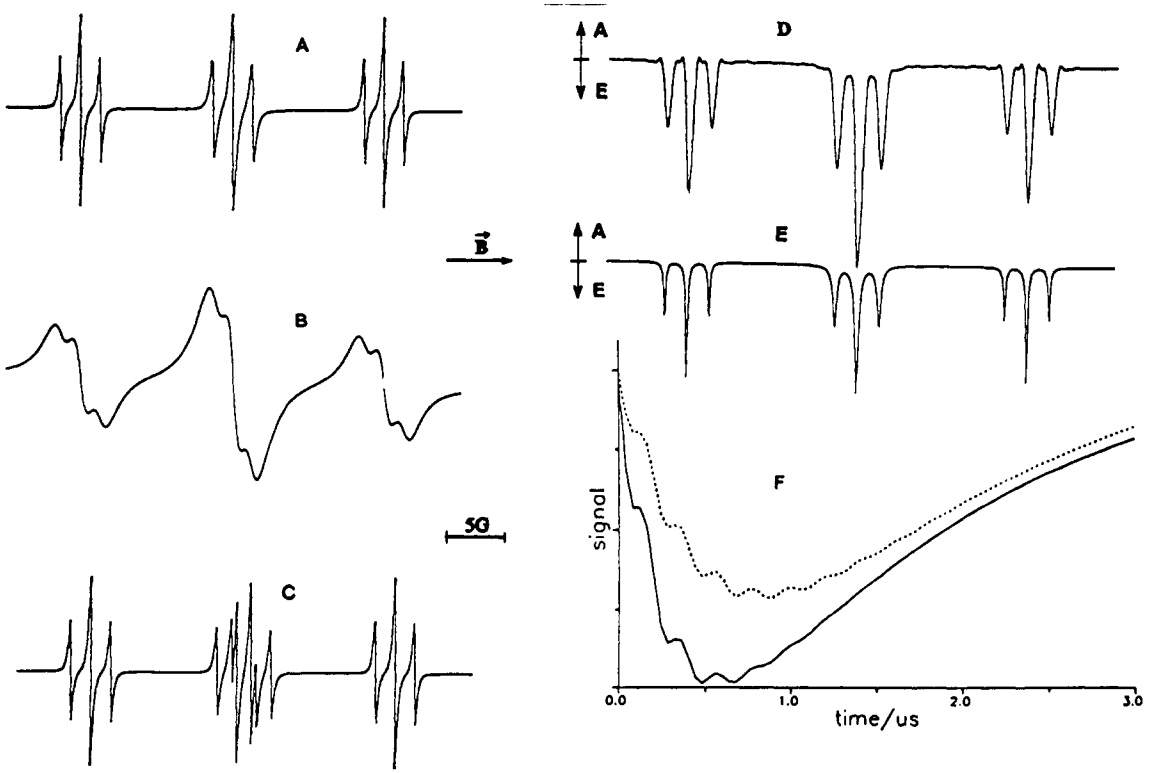

Figure 8. Theoretical 100-kHz and TR ESR spectra associated with the hindered rotation in the methylene fragment. Hfcc constants used: 6 and 21 G for the methylene protons and 1.7 G for the *m*-protons. (a–c) ESR spectra (100 kHz) as a function of line width and exchange rates: (a) $k_{12} = k_{21} = 4 \times 10^9$ s^{-1} and line width = 0.3 and 1.5 (b) G; (c) $k_{12} = 5 \times 10^{10}$ s^{-1}, $k_{21} = 5.8 \times 10^{10}$ s^{-1} and line width = 0.3 G; (d–f) simulated TM-polarized TR ESR spectra with $k_{12} = k_{21} = 4 \times 10^9$ s^{-1}, Rabi frequency of 0.5 rad MHz, $T_1 = 2$ μs, $T_2 = 0.5$ μs (calculated with 128 points FFT, 40-ns resolution) at delay time of (d) 0.3–0.6 μs and (e) 1–2 μs; (f) time evolution of magnetization of lines with $M_I = 0$ (solid line) and $M_I = \pm 1$ (broken line).

dominated spectra are commonly observed.[4,14] Apparently, the reactions between the polarized triplet initiator and the phenolic quenchers are much slower than with other phenols. Even more intriguing is the observation of the identical asymmetry in the $M = \pm 1$ lines, which are expected to be only slightly dependent on the Δg-mechanism. Indeed, the difference in the *g*-factors between butylated phenoxy radicals (2.0045) and ketyl radicals such as BPH (2.0030) and PAH (2.0037) can account for only 5–10% of the deviations from the symmetry for the lines. In the PA/IOH system the lines from the PA ketyl radical do not exhibit any single-phase TM contribution (which would have been absorptive[15]), yet the polarizations of the $M = \pm 1$ lines are the same as those in the BP/IOH system. This suggests that the TM contribution derives from the photolysis of a product generated in the secondary photochemical reactions, acting as a (triplet) photosensitizer.

Furthermore, the signal intensities increased with decreasing flow rates, consistent with the proposed accumulation of quinoid products of the radical disproportionation which are good secondary photoinitiators. Observation of CIDEP spectra due to such secondary product photolysis has been reported;[9,16] in general, this process plays a more important role if the metastable products are more reactive than the parent initiators. Common manifestations of the effects of such secondary photolysis are unexpected signs of TM contributions, the dependence of the polarization pattern on flow rates, viscosity, and chemical scavenging reactions affecting the yields of the photoproduct. Indeed, in simultaneous measurements we have observed a parallel behavior between the increase in the relative intensity of the broad component in CIDEP spectra and the homogeneous line broadening in 100-kHz ESR spectra at increasing flow rates in one 2,3-diphenylbenzoquinone/IOH system.

In order to eliminate any possible TM contributions from the parent photoinitiators, TBP was used, and the TR ESR results are shown in Figure 4b,c. The totally emissive signal observed can arise only from photolysis of a secondary product. Furthermore, the intensity pattern of the methylene protons clearly is not 1:2:1 (Figure 4c). At early detection (0.2–0.5 μs) the spectrum is 1:2:1. At longer delay times (0.5–1 μs) it changes to 1:1.5:1 and finally to 1:1:1 at 2-μs delay time as in the 100-kHz modulated ESR observation. The same behavior was also observed in the photolysis with chlorine as the initiator (Figure 5c,d). Here the intensity of the central line in the TR spectra was further reduced to 1:1.1:1 compared with those of the TBP system (1:1.5:1 detected at 1-μs delay) but still much greater than the 1:0.5:1 pattern (Figure 5b) in the simultaneously detected 100-kHz spectra. Both polarization patterns clearly demonstrate the effects of rotational hindrance in the radicals, proposed to consist mainly of **XO**. Furthermore, the spectra give some indication of hindered rotation also in the primary radical as the TM-polarized **IO** (in lower concentrations) contributes to the observed signals.

The polarization of the second broad and unresolved component seemed to be also E^*/A for PA, AP, and 2-acetylfuran. This broad and unresolved signal can be assigned to the primary **IO** radical affected by H-exchange. Based upon the theoretical treatment given in the appendix, our calculations show that in the first 0–3 μs the broadening of the TR ESR spectra would be comparable to those observed in the 100-kHz spectra. RPM contribution (in presence of degenerate H-exchange) broadens the spectra in a different manner,[17] and the overall feature of the signal will be predominantly single-phase with its sign being

(14) Depew, M. C.; Wan, J. K. S. In *The Chemistry of Quinoid Compounds*; Patai, S., Rappaport, Z., Eds.; J. Wiley and Sons: New York, 1988; Vol. 2, Part 2, Chapter 16, p 963.

(15) Shushin, A. I.; Depew, M. C.; Wan, J. K. S. *Res. Chem. Intermed.* **1991**, *16*, 165. Craw, M. T.; Depew, M. C.; Adrian, F. J.; Wan, J. K. S. *Bull. Chem. Soc. Jpn.* **1989**, *62*, 1308.

(16) Shkrob, I. A.; Wan, J. K. S. *Res. Chem. Intermed.* **1992**, *17*, 77.

(17) Batchelor, S. N.; Heikkila, H.; Kay, C. W. M.; McLauchlan, K. A.; Shkrob, I. A. *Chem. Phys.* **1992**, *162*, 29.

dependent on the interplay of Δg-RPM and TM mechanisms. In the CIDEP spectra of the BP/**IOH** system (Figure 3e), no such broad component is observable. This lack may be due to a signal exhibiting a purer two-phase contribution, as in the case of extreme broadening, a superimposition from a two-phase polarization is even more difficult to detect than those from an E^*/A polarization.

Thus, the TR ESR observations are consistent with the proposed scheme and further confirm the usefulness of TR ESR for studying exchange and interconversion phenomena taking place on the hyperfine time scale.

(c) The Case of a Phenoxy Diradical. While we have been able to account for most of the experimental observations by proposing the formation of a rotationally hindered **XO** radical, we have also considered the possible formation of some form of a diradical via further photooxidation of the primary **IO** radical. In an earlier study,[3] (chemically generated) diradicals from 1,3,5-tris(3,5-di-*tert*-butyl-4-hydroxyphenyl)benzene, in which the three phenoxy/phenolic groups are directly conjugated with the central benzene ring, were characterized as triplets with rather weak ZFS of about 40 G. However, in the time average the distance between the oxygen atoms of the phenolic groups in **IOH** are expected to be 2–3 Å bigger than in that triphenol, and, hence, the isotropic magnetic interaction between the two electrons (exchange integral J) as well as the ZFS of a potential diradical would be substantially smaller. Yet, no such species was observed for **IOH**, even during photolysis at 77 K. If the aforementioned superimposition from **X'O** in the well-resolved CW-ESR spectra were interpreted in terms of splittings ($\leq$1.7 G) evoked from delocalization of the two unpaired electron spins in a diradical of **IOH**, the exchange integral J would therefore be $\leq$1.7 G. Figure 9 shows the simulated ESR spectra of such diradicals ($J \leq 1$ G) at different rates of spin exchange. They do not fit our experimental observations. We have therefore concluded that diradicals are not formed in the **IOH** system. Possibly, this is due to the reactive nature of the primary **IO** radical and thus it reduced lifetime as compared to some of the well-known persistent ortho-substituted phenoxy radicals.

4. Theoretical Treatment of the Exchange Phenomena in the *p*-Oxy-*m*-di-*tert*-butylbenzyl (OTBB) Moieties and Their Manifestation in ESR and CIDEP

The rotational interconversion in our system may be considered as hopping between two sites, **1** and **2**, as already mentioned. In the state **1** the hfcc on the first nucleus is A_1 and the hfcc on the second nucleus us A_2, and in the state **2** this is reversed. We began with a modified Bloch equation for such a system:

$$d\mathbf{M}_k/dt = \mathcal{L}_k\mathbf{M}_k + (1/T_1)\mathbf{M}_{eq,k} \pm (k_{21}\mathbf{M}_2 - k_{12}\mathbf{M}_1) \quad (1)$$

where $\mathbf{M}_k = (\mathbf{M}_{kx},\mathbf{M}_{ky},\mathbf{M}_{kz})$, $k = 1, 2$ is the magnetization of radical in the k-th state (here we accept that the z-axis of the rotating frame coincides with the direction of the external magnetic field), $T_{1,2}$ are the relaxation times, k_{12} and k_{21} are the rate constants for hopping between the states, and $\mathbf{M}_{eq} = (0,0,P_{eq})$ is the Boltzmann population magnetization. $\mathcal{L}_k$ is the corresponding Bloch matrix,

$$(\mathcal{L}_k)_{zz} = -1/T_1;\ (\mathcal{L}_k)_{xx,yy} = -1/T_2;$$
$$(\mathcal{L}_k)_{xy,yx} = \pm\Delta\omega_k;\ (\mathcal{L}_k)_{yz,zy} = \pm\omega_1 \quad (2)$$

Here ω_1 is the microwave field in the frequency units (or Rabi frequency), $\Delta\omega_k = \omega - \omega_k$ is the offset, ω is the magnetic field in the frequency units, and ω_k are the resonance frequencies for the corresponding states (at equal orientation of the nuclear spins). Equation 1 has to be solved for all nuclear states of the system, and a sum

$$\mathbf{M}_y(t) = \sum\nolimits_{conf}(\mathbf{M}_{1y} + \mathbf{M}_{2y}) \quad (3)$$

is proportional to the detected CIDEP signal.[4] At the instant of a laser pulse leading to radical-pair formation ($t = 0$) the nonzero

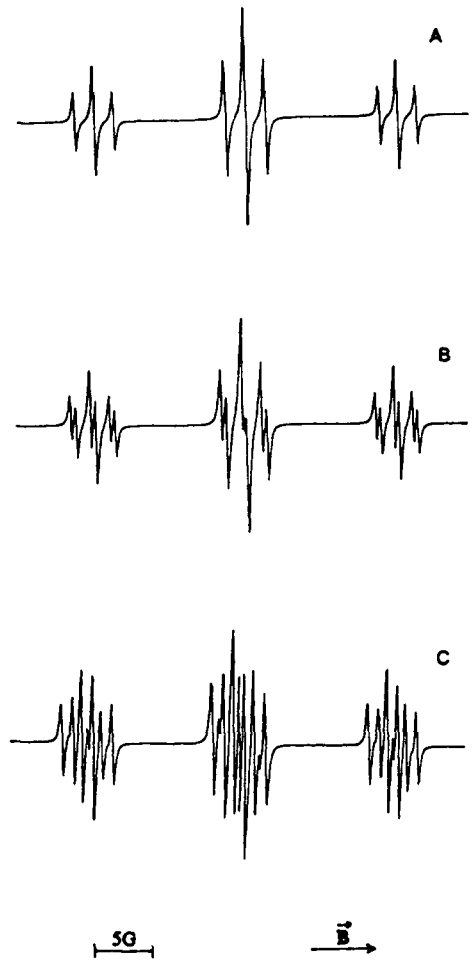

Figure 9. Simulated spectra diradicals from **IOH** with hfcc of 13.2 and 1.7 G for the methylene and *m*-H, respectively. Spin exchange between the unpaired spins is taken as (a) 0 G, (b) 0.5 G, and (c) 1 G. Line width is 0.2 G.

z-components of the magnetizations $\mathbf{M}_{1,2}$ are

$$\mathbf{M}_{1z}(t = 0) = k_{21}(P_1/(k_{12} + k_{21})) \text{ and}$$
$$\mathbf{M}_{2z}(t = 0) = k_{12}(P_2/(k_{12} + k_{21})) \quad (4)$$

where $P_{1,2}$ are the corresponding initial polarizations in the states 1, 2 for a given orientation of nuclei.

In the above simplified treatment of the spin dynamics in the system, we have assumed that (i) generation of the initial polarization is very fast relative to the rotation rates, (ii) there are no secondary reactions of the radicals comprising the pair, and (iii) interradical exchange is negligible. The depletion of the radicals via first-order reactions may be accounted for indirectly by changing the T_2 time, provided that $P_{1,2} \gg P_{eq}$, and thus $\mathbf{M}_{eq}$ becomes 0.

Introducing a vector $\mathbf{M} = (\mathbf{M}_1,\mathbf{M}_2)$ and taking into account a linearity of eq 1, we can rewrite it in the generalized form,

$$d\mathbf{M}/dt = -L\mathbf{M} \quad (5)$$

or in the Laplace transformed form,

$$\mathbf{M}(t = 0) = (sI + L)\mathbf{M}(s) \quad (6)$$

Numerically, the fastest way to solve eqs 1, 5 is first to solve the 6 × 6 linear complex matrix eq 6 for a series of imaginary $s = 2\pi i\nu/N\tau, \nu = 1, ..., N$ by using the Gauss elimination algorithm and then to perform a Fourier transformation of $\mathbf{M}(s)$ to the time domain (using standard FFT procedure). This method allows us to avoid scaling problems due to thousand-fold differences between $k_{12,21}$ and rates of the relaxation and the microwave-induced

transitions. The convergence was found to be achieved at N = 128–512 and τ = 20–50 ns. This algorithm proved to be faster than a numerical finding of eigenvalues and eigenstates of matrix L, not to mention the step-by-step time integration of eq 5.[17] Next, we shall consider the physics of the CIDEP development at interconversion.

A nonequilibrium polarization in radicals has two common origins: the triplet mechanism (TM) and the radical-pair mechanism (RPM ST_0). The first mechanism is a transfer of the polarization from the reacting phototriplet to the resulting radicals, and, therefore, the polarization of the latter is an enhanced thermal polarization, with the signs of polarizations either both positive or both negative. When the hfcc in the methylene fragment of the radical is the largest, a 1:2:1 ratio in the hyperfine line intensity pattern will be observed under conditions of rapid exchange. By contrast, for a triplet-born pair with equal g-factors of the radicals, the RPM ST_0 results in a −1:0:1 ratio between the lines. Some slight deviations from this antiphase spectrum are theoretically possible either due to a difference in g-factors (in this case intensities of the lines with nonzero overall spin projection M of methylene protons are very close to those at $\Delta g = 0$, but the central line is nonzero[4]) or due to the so-called RPM ST_- mechanism. The latter corresponds to the situation when the radicals are drifting apart so slowly that adiabatic transitions from the singlet to the lowest triplet state occur (RPM ST_-).[4] Such a mechanism usually becomes dominant for radicals with very large hf splittings and/or sometimes when the radical diffusion is greatly impeded in very viscous solutions. Although we would not expect the ST_- mechanism to play a significant role in the present system, its contribution would have produced a −1:−1:0 distortion which may again be treated as a sum of −1:0:1 and −1:−2:−1 signals.

A striking feature of the antiphase RPM ST_0 polarization in the system is its complete independence of the exchange rate. Indeed, since $(\alpha\beta)$ and $(\beta\alpha)$ nuclear subensembles carry polarization of opposite signs in different sites, the resulting spectrum is entirely independent of the exchange rate due to a compensation of these contributions. Thus, in principle the exchange phenomenon cannot be observed in the RPM-polarized pattern of the methylene fragment. We must emphasize that this conclusion in the present system is not general for chemical exchange in TR ESR, as RPM has been shown to strongly affect lines of higher multiplets[4,5] in radicals with more complex spectra.

On the other hand, the polarization from TM (or any other mechanisms giving a 1:2:1 pattern[4,18]) must be influenced by the exchange to the same extent as in the modulated ESR spectra. At $k_{12} = k_{21}$ (equivalent conformations), the modulated spectra in the experiments are shown to become more and more 1:0:1 in character with decreasing exchange rates. The central line (M = 0) is not only smaller in amplitude than the outer ones (M = ±1) but is also much broader. It is important to note that the reduction in the intensity of the central line at the given exchange rate depends on the transverse relaxation time: the higher T_2^{-1}, the smaller the effect of the exchange, as demonstrated in the experimental observations described. This effect is partially responsible for a remarkable feature of the TM-polarized time-resolved spectra, which is that the relative intensities of the lines are functions of time delay, going from a 1:2:1-like polarized pattern to a more 1:0:1-like modulated ESR spectrum. At first glance, this transformation should occur on the time scale of the reciprocal constants $k_{12,21}$. In reality, however, a finite time of the rotation of magnetization from z-direction (the laboratory field) to the xy-plane (at which it is detected) results in the broadening of the lines and the so-called Torrey oscillations both in the field and time domains.[4,13] These transient phenomena effectively destroy a coherency needed for the redistribution of magnetic polarization through the exchange at $t \leq 1/\omega_1$. Consequently, a relative reduction and broadening of the central line occurs only at longer times. Thus, *exchange in the time-resolved TM-polarized spectrum may be fingerprinted by a time dependence of the relative intensities of lines.* Exchange as a result of conformational interconversion in CIDEP has previously been considered in the RPM ST_0 polarized cyclohexanolyl radicals.[5] In that work the spectrum consists of five lines with incomplete compensation for the noncentral lines, and the exchange effects on the lines with $M = \pm 1$ can be readily seen. For the present systems with hindered rotation in the methylene fragment, the results are rather different: no exchange effects were seen in the RPM contribution, and the effects on the TM polarization may be rather small at early detection times. Thus, the spectral features of the system may be practically indistinguishable from that of free rotation unless its time dependence is analyzed. The uniqueness of time-dependent, time-resolved ESR techniques should add another dimension in the studies of radical dynamics.

Acknowledgment. This research is supported by the Natural Sciences and Engineering Research Council of Canada under the Networks of Centres of Excellence program and by DuPont, Canada. One of us (P.E.) wishes to acknowledge the award of a Postdoctoral Fellowship from the Swiss National Science Foundation.

(18) Blättler, C.; Jent, F.; Paul, H. *Chem. Phys. Lett.* **1990**, *166*, 375.